

Study of Physicochemical Properties of PVC Thin Films Affected by Carbon Nanotubes to Prevent Photodegradation During UV Light Exposure

R. M. Dadoosh¹, A. F. Alwan¹, S. A. Farhan¹, B. Essam Jassim², A. Mahmood¹, L. Ghaeb Al-Saadi¹, R. N. Abed^{*3}

¹ Polymer Research Unit, College of Science Al-Mustansiriyah University, P.O. Box: 10052, Baghdad, Iraq

² Middle Technical University Institute of Technology, P.O. Box: 50405, Baghdad, Iraq

³ Department of Mechanical Engineering, College of Engineering, Al-Nahrain University, P.O. Box: 64040, Jadria, Baghdad, Iraq.

ARTICLE INFO

Article history:

Received: 13 Jan 2024

Final Revised: 17 Feb 2024

Accepted: 21 Feb 2024

Available online: 06 Mar 2024

Keywords:

PVC

UV stabilizer

Adopted polymer

Carbon nanotube

Surface morphology

ABSTRACT

This study investigates the impact of carbon nanotubes on the structure of poly(vinyl chloride). Carbon nanotubes derived from corn cobs (1 g) and molten sodium hydroxide (3 g) at a weight ratio of 1:3 were used as additives. These doped poly(vinyl chloride) samples were analyzed. Different concentrations of carbon nanotubes (0.25, 0.50, and 0.75) were incorporated into the poly(vinyl chloride) lattice. The effects of these additions demonstrated remarkable resistance to continuous ultraviolet light exposure, effectively countering photodegradation. Before introducing the nanoparticles, volatile substances generated free radicals, leading to reduced weight and molecular weight in PVC thin films. To counteract degradation, stabilizers were introduced to the polymer. Photostability was achieved by doping PVC with carbon nanotubes, with monitoring of carbonyl groups (I_{CO}), polyene ($I_{C=C}$), and hydroxyl (I_{OH}) growth against irradiation time. Upon adding carbon nanotubes, I_{CO} values increased from 0.16 to 0.24, and $I_{C=C}$ values rose from 0.17 to 0.28. Conversely, I_{OH} decreased from 0.14 to 0.058, mitigating photodegradation. Crystalline size and micro-strain were calculated. The study also tracked surface morphology and weight loss changes in nanocomposite PVC thin films upon irradiation. The findings demonstrated the effective UV-blocking capabilities of carbon nanotube-PVC blends, providing substantial protection to thin films. Additionally, weight loss calculations, polymeric thin film surface changes, and viscosity assessments were conducted. Prog. Color Colorants Coat. 17 (2024), 307-324 © Institute for Color Science and Technology.

1. Introduction

Since the early beginning of the Industrial revolution in the 1930s, poly(vinyl chloride) (PVC) has a single of the very charming polymers whose production witnessed huge growth over the years [1]. The capacity of poly(vinyl chloride) on a global scale amounted to about

a lot of reached 80 tons in 2021. Plastic is an excellent replacement in building construction, where it can use as a replacement material to compensate for heavy metals that are subjected to corrode and glass matter that is easily breakable [2, 3], due to its excellent properties as durability, and low costs of manufacturing [4].

*Corresponding author: * rasheed.n.abed@nahrainuniv.edu.iq
<https://doi.org/10.30509/pccc.2024.167260.1275>

PVC is utilized in electronics production, automobile components, medical products, office equipment, sports materials, plastic cards, and packaging. Therefore, is used in many applications such as the manufacture of tubes, cables, threads, and connections of piping in electricity in addition to water [5].

Nowadays, PVC in both forms (hard and elastic) is produced in large quantities in China and in less range in other regions in the world like India and Middle East countries [5]. The hard form of PVC is extremely used in building materials (doors and windows) and packaging [5]. While a soft form of PVC is used in manufacturing cable insulation [6]. Usually, PVC is a white, strong, and solid polymer that is soluble in tetrahydrofuran (THF) [7]. In spite of these fascinating features, PVC has poor photostability against UV light [8], especially for outdoor applications [9]. This problem has a very bad impact on PVC properties leading to changes in chemical composition and structural organization. The degradation process starts when hydrogen chloride (HCl) eliminate from the PVC leading to a formation of long polyene chains and chlorine radicals [10], the elimination of HCl causes a change in the mechanical and physical properties [11, 12] and generates micro-splitting, the oxidative reactions take place on the exterior surface of PVC, in the attendance of oxygen, driving to the chains split and the small fragments creation which destroys the properties of the material [13]. The Schiff base of the melamine moiety unit was mixed with PVC lattice to be modified, and then copper oxide was blended with modified PVC to reinforce its structure from the dehydrochlorination, and be photostability against the UV light that causes degradation process [14]. On the other hand, this elimination causes harm to the ecology system since the resultant HCl has a corrosive effect, therefore a dehydrochlorination process in PVC leads to chains crosslinking and causing discolored and brittle [15]. So, to deal with this problem of polymer ionization by UV irradiation causes electronic excitation leads to a rupture of polymer structure that affects bonds between atoms and there are several solutions appear to be useful to avoid photodegradation for example, using stabilizers which are chemical compounds that are used to keep the PVC flexibility, strength, and toughness; these compounds are usually added to the polymers to hinder the degradation process and extend their life time [16].

Therefore, can transform the harmful ultra violet radiation to thermal energy, which is faded through the

polymer template [17]. Stabilizers involve broad spectra of compounds including, antioxidants, fire retardants, and blowing reagent [18]. Many mechanisms are predicted about how the additives can stabilize PVC, for example, radical scavengers, (UV) absorbers [19], and HCl scavengers [20]. Therefore, PVC can be used in outdoor applications to be resistant to photodegradation and photooxidation to elongate its lifetime by reinforcing its structure, thereby, one of these stabilizers is a carbon nanotube (CNT), it has a hexagonal arrangement of carbon atoms with has nanometer-scale rolled up into a thin, long, cavity cylinder [21]. It has extraordinary mechanical, electronic properties, and high thermal stabilization [22], which make it ideal in wide applications like biomedical application [23], energy management [24], material science, and electronics [24]. Carbon nanotubes (CNT) have higher tensile strength reach to about 100 times compared to steel [25]. Because of their nanometric scale, dimensions, and the high proportion between the length and diameter of the particles, carbon nanotubes are ideal for applications that demand highly specific surfaces, such as reinforcing agents in materials composites [26]. Furthermore, CNT is strengthening PVC which can transform the nanocomposite thin film of PVC to be high bearing when exposed to a high temperature in the outside environment [27].

Herein, in the present work, the fabrication of a nanocomposite thin films of PVC with different concentrations of Carbon nanotube (CNT) (0.25, 0.50, and 0.75). Carbon nanotube (CNT) has been confirmed as a photostabilizer of PVC. These nanoparticles from CNT were used to study their outcome on the photodegradation of PVC lattice. The PVC stabilization is to prevent and liberate hydrogen chloride (HCl) from the PVC, in addition, strengthen the mechanical and physical properties.

The present work focuses on adding CNT to the PVC lattice will improve the absorbance of UV light and decrease the reflectance, thereby, ensuring the effect of CNT to resist the photodegradation of PVC thin film. Also, the FESEM images illustrated the surface morphology and the surface roughness. The nanocomposite thin films of PVC with CNT (0.25, 0.50, and 0.75) were used in many applications such as electronics, automobile components, medical products, office equipment, sports materials, plastic cards, packaging, and used in many outdoor applications such

as the manufacture of tubes, and fittings of piping in electricity.

2. Experimental

2.1. Materials and method

The PVC material was bought from the company Istanbul, Turkey (PetKim Petrokimya), where the carbon nanotube (CNT) has been synthesized in the lab.

2.2. Characterization techniques devices

The scanning electron microscope images (SEM, 3 nm at 30 kV SE, S50 with a low vacuum) were utilized to demonstrate the profile of the CNT fibers. The samples of PVC/CNT were checked by the device of reflectance Avantes (DH-S-BAL-2048, UV-Visible Spectro-2048) at the ranging of wavelength as of (250-1300 nm) for a step wavelength 0.5 nm. The microscope of atomic force (AFM, AA2000) device is utilized to allocate the roughness for the blank PVC and PVC/0.25 CNT, PVC/0.50 CNT, and PVC/0.75 CNT nanocomposite thin films. It is used to illustrate the surface morphology. QUV tester used the irradiation of the samples under UV light.

2.3. Carbon nanotube synthesis (CNT)

Corn cobs (1 g) were used as constituting principal to

prepare CNT mixed with (3 g) of molten sodium hydroxide at a percentage ratio (1:3 wt. %), then placed in a furnace for burning at a temperature of 550 °C for an hour and the temperature increases 10 °C gradually. The composite that resulted from burning was cooled at room temperature, and then cleaned numerous times with hot water, hydrochloric acid, and distilled water to remove any remaining content of NaOH until reached the achieved pH desired of (7.0). After that, the moist bulk went through a 12 h drying process at a temperature of 80 °C in the oven. The CNT resulting achieved from the above process was inspected by SEM to show the shape of the CNT fiber as shown in Figure 1.

2.4. Preparation of PVC doped with CNT

2 g of PVC blank was dissolved in 100 mL of tetrahydrofuran (THF) and added carbon nanotubes (CNT) with different percentages (25, 50, and 75 wt. %) to the solution. The solution of PVC with different concentrations of CNT (0.25, 0.5 and 0.75) mixtures was stirred for 2 h to produce a homogeneous solution. The casting path was utilized to make four different nanocomposite thin films in a dish of glass measuring 4 by 4 cm as, the procedure of synthesis of the CNT and preparing the nanocomposite thin films of PVC with CNT as shown in Scheme 1.

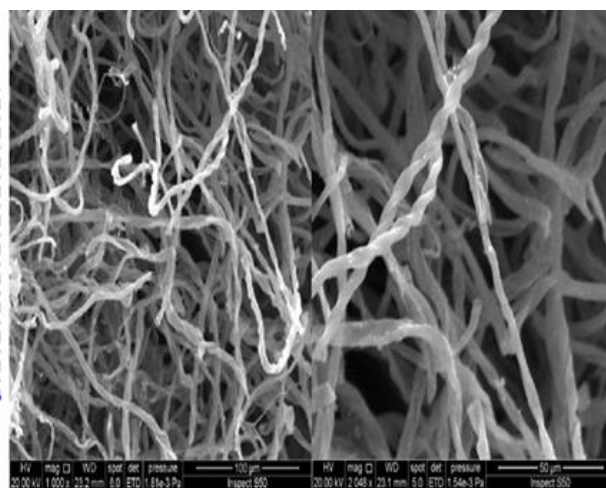
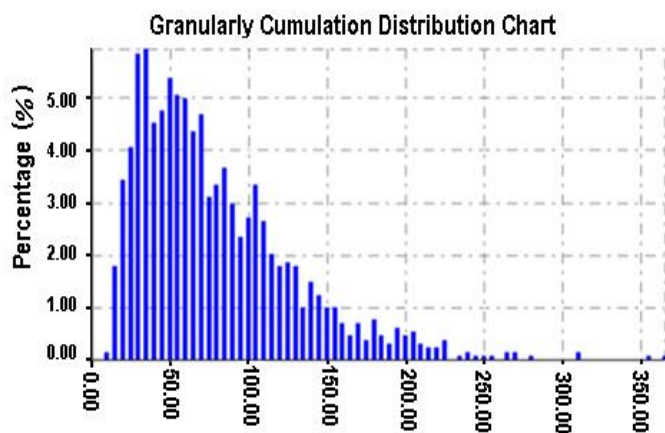
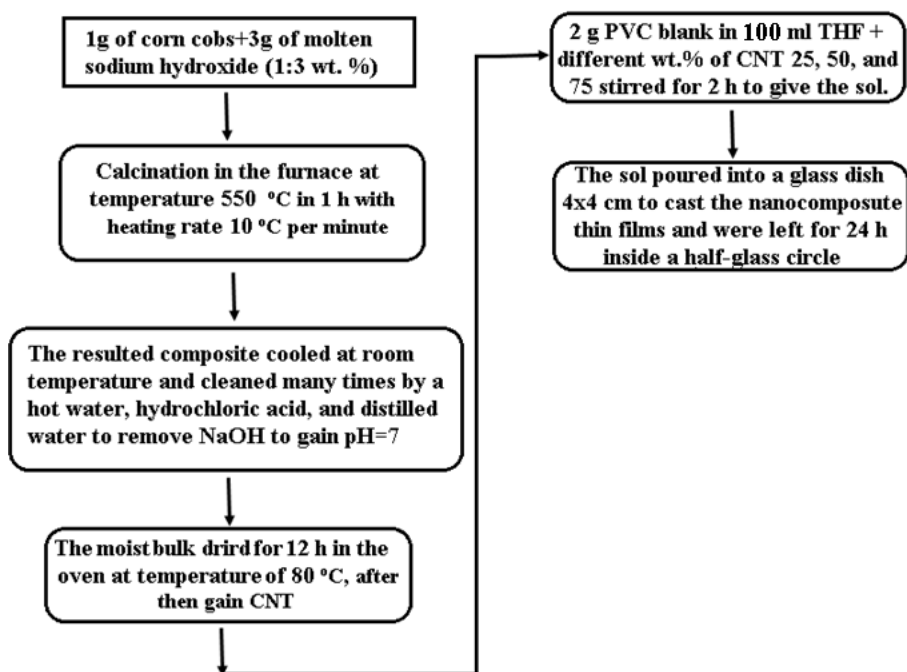


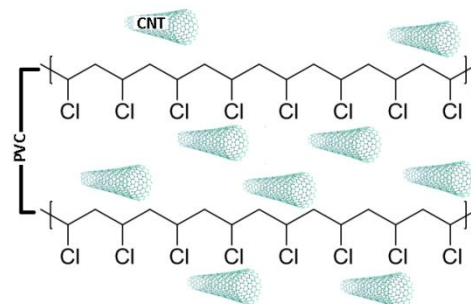
Figure 1: SEM image that illustrates the shape of the CNT fiber.



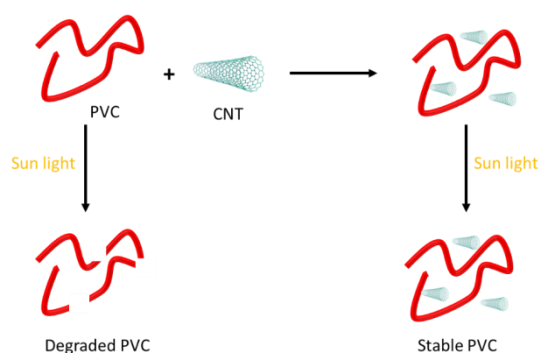
Scheme 1: The descriptive flowchart to explain the synthesis of CNT and prepared the nanocomposite thin films of PVC with CNT.

The graphical abstract of the PVC illustrates the exposure to sunlight and degradation from the sunlight before reinforcing it. After being reinforced by CNT, the PVC structure has strengthened and stabilized as shown in Scheme 2.

The last thin film's thickness was measured by digital vernier and it was near 50 μm . The thin films were left for 24 h in an interior half-glass circle shield at room temperature to dry and be ready for examination. Therefore, Scheme 3 shows the CNT fiber inside the series of PVC structure as a descriptive graphical.



Scheme 3: CNT inside the PVC structure.



Scheme 2: Degradation of PVC with sunlight and after reinforced by CNT to be stable.

2.5. Display the PVC thin film to UV light

Both PVC blank and samples of the nanocomposite thin films of PVC with CNT have been exposed to radiation for irradiation utilizing a QUV tester. The UV light with a wavelength range of about 313 nm was employed. The samples were exposed to UV light for a range of a lot of times from 50 to 300 h at intervals of 50 h. To guarantee the equal arrival of UV light to the samples from all directions, the samples were rotated at regular intervals. Due to the ozone layer's ability to block out the majority of UV light from solar energy, UV light was applied for 300 h to simulate sunlight for a full year. Figure 2 displays the irradiation of samples that are exposed to UV light radiation by using a QUV tester and depositing them inside the tester.



Figure 2: QUV tester and the samples inside it.

3. Results and Discussion

The results and discussion focused on how blending CNT into the PVC lattice will improve the absorbance of UV light and decrease the reflectance, thereby, ensuring the effect of CNT to resist the photodegradation of PVC thin film.

3.1. XRD

The techniques that are most common for verifying the formation of nanoparticles are to identify the crystalline shape and the size of the crystalline particles as shown in the XRD pattern of Figure 3. The peaks that are found to be sharp and separate from each other, the material is considered crystalline, but if the peaks are broad and overlapping, then the material is considered amorphous. The crystalline through Miller

coefficients, we can know the crystalline form of the nanomaterial, which are values derived from the crystalline intersections of the crystalline face. To express its relationship to the crystalline axes, through which the crystalline form can be distinguished if it is cubic, cylindrical, or any other shape [11]. Therefore, through the Scherrer equation, the crystalline size can be calculated from the equation 1 [28]:

$$D = \frac{0.9 \lambda}{\beta \cos \theta} \quad (1)$$

Where, D: crystalline size, λ : X-ray wavelength (diffraction wavelength), β : full width at half maximum (FWHM), and θ : diffraction angle.

Figure 3 shows the index of XRD diffraction lines of the CNT nanoparticles after synthesis. The crystalline structure shape of CNT coincides with the reference [29].

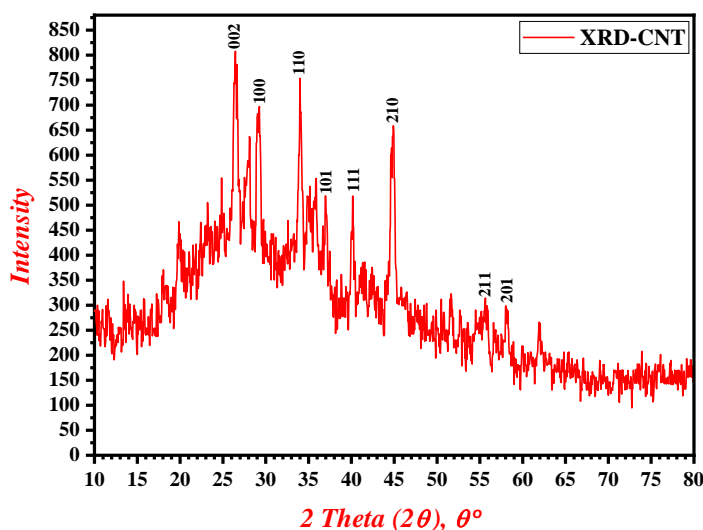


Figure 3: XRD of the CNT pattern.

Likewise, the microstrain should be calculated from equation 2 [30]:

$$\varepsilon = \frac{\beta}{4 \tan \theta} \quad (2)$$

Where, (ε) is the microstrain, (β) is FWHM, and (θ) diffraction angle. It can see from Figure 3 many parameters are shown in Table 1.

3.2. Absorption coefficient of blank PVC and PVC with CNT blended

The absorption coefficient (α) of the samples (blank PVC and PVC with CNT) is very important to

determine the value of absorption through the UV region. Therefore Figure 4 shows the regions that have high absorption in the UV region between the wavelength values. For the blank PVC, the maximum absorption falls in the wavelength region ($\lambda \geq 290$ nm), while the maximum absorption for the PVC with CNT (0.25, 0.50, and 0.75) falls in the wavelength region between ($\lambda \geq 380$ nm) before declines in the visible region [30].

Therefore, the nanocomposite thin films showed high absorption of the UV light region, this a good indication for these samples to absorb the UV light after added CNT.

Table 1: XRD properties of the CNT pattern and microstrain.

Pos. $2\theta^\circ$	Height [cts]	β (FWHM)	d-spacing [Å]	Rel. Int. [%]	Tip Width	$\varepsilon \times 10^{-3}$ (Micro-strain)
26.452	469.62	0.492	3.370	100.00	0.590	9.134
29.146	370.65	0.394	3.064	78.92	0.472	6.606
34.056	429.25	0.394	2.633	91.40	0.472	5.608
37.045	200.00	0.590	2.427	42.59	0.708	7.689
40.122	224.04	0.394	2.247	47.71	0.472	4.703
44.828	399.04	0.492	2.022	84.97	0.590	5.205
55.199	59.089	0.085	1.664	13.37	1.417	0.710
58.049	92.618	0.388	1.589	17.41	0.945	3.053

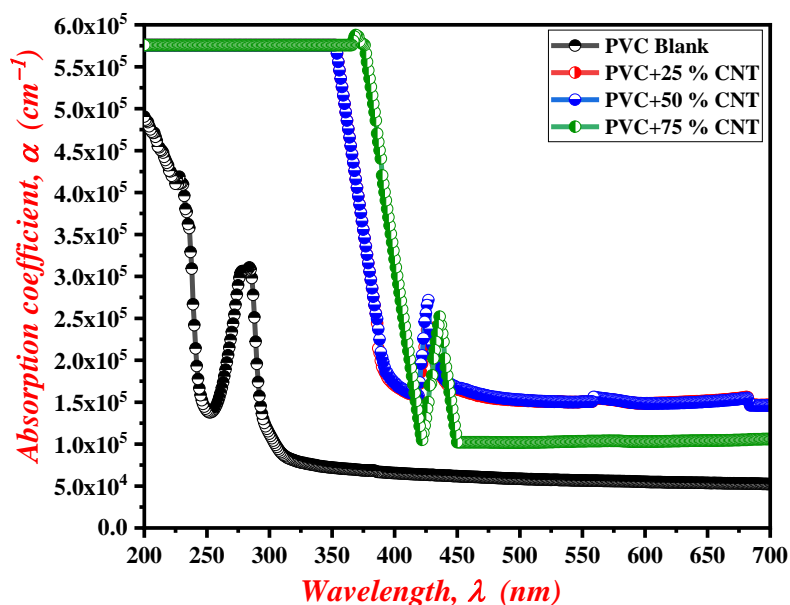


Figure 4: The absorption coefficient of blank PVC and PVC with CNT blended.

3.3. Reflectance of blank PVC and PVC with CNT blended

The reflectance (R) factor is regarded an indicator to illustrate the value of reflectance (R) for the blank PVC and PVC with CNT blended as shown in Figure 5.

Therefore, it can be seen from Figure 5, that the reflectance (R) of blank PVC bigger than the PVC with CNT blended, where the reflectance (R) value is near to a value of 0.22 through the the wavelength of UV region between ($200 \geq \lambda \geq 300$ nm). And then, after adding the CNT (0.25, 0.50, and 0.75) to the PVC the value of reflectance (R) declined remarkably through the wavelength region between ($200 \geq \lambda \geq 390$ nm), this proves that PVC/CNT nanocomposite thin films have been absorbed the UV radiation remarkably, where after added CNT to the PVC structure is decreased the reflectance value [30].

3.4. UV irradiation effect on weight loss of PVC

In the presence of light, heat, and moisture, PVC dehydrochlorinates autocatalytically. Discoloration, unsaturated fragmentation, significant mechanical and physical property changes, minimizing molecular weight, and weight loss all result from the elimination of hydrogen chloride (HCl). These uncomplimentary modifications are brought on by chain scission and cross-linking. Loss of weight is a sign of photodegradation to PVC. As a result, the PVC thin

films were weighed at various times prior to being exposed to UV light (W_0), and they were then reweighed at 50 hours later (W_1). Pure PVC and PVC blends with CNT of the thin film weight loss (%) are calculated using equation 3 [26].

In Figure 6 explains the weight losses (%) curves at different irradiation times for several samples of blank PVC and PVC/CNT [31].

$$\text{Weight loss (\%)} = \frac{W_0 - W_1}{W_0} \times 100 \quad (3)$$

Figure 6 illustrates how the time of irradiation affected the PVC films' weight loss. Unquestionably, the CNT additives were very important in stabilizing PVC. During the first 50 hours, weight loss was increased rapidly; however, after that, it steadily increased gradually. The CNT that additives to the PVC lattice lead to decrease the weight loss of the nanocomposite thin films of PVC with CNT comparison with blank PVC. the decreased in PVC photodegradation due to adding CNT (0.25, 0.50, and 0.75). Therefore, from Figure 6, the weight loss escalated for the blank PVC and lower loss for the nanocomposite thin films of PVC/CNT. It can see from Figure 6 the weight loss values of blank PVC, PVC/0.25 CNT, PVC/0.50 CNT, PVC/0.75 CNT were 0.98, 0.57, 0.50, and 0.40, respectively, all these values after 300 h of irradiation [32].

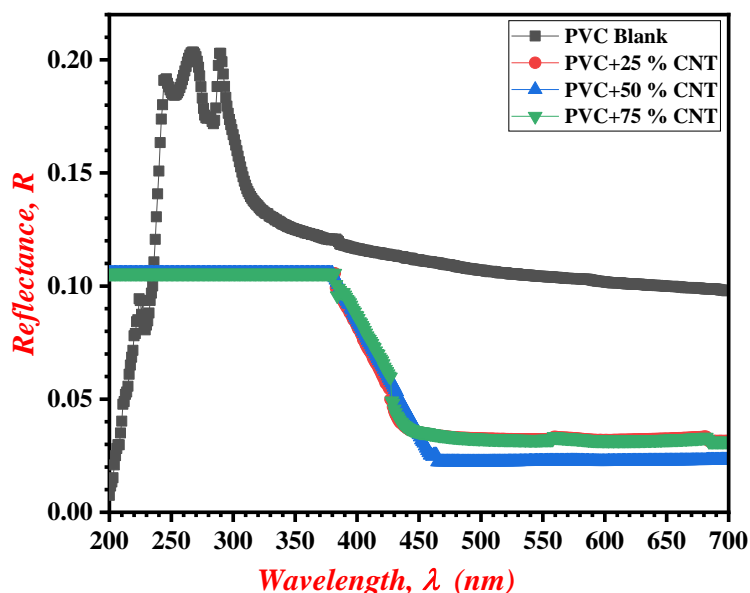


Figure 5: Reflectance of the PVC and PVC with CNT blended.

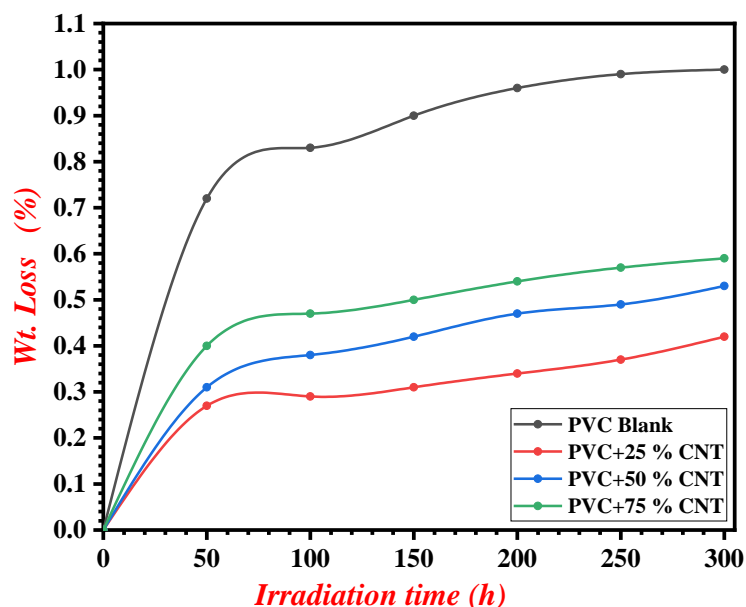


Figure 6: Weight loss percentage as a function of irradiation time of blank PVC and PVC with CNT blended.

3.5. UV irradiation impact on FTIR spectroscopy of PVC

The chains of the FTIR analysis for the nanocomposite thin films of blank PVC and PVC with CNT (0.25, 0.50, and 0.75) are shown in Figure 7. The removal of HCl from the polymer chain causes the generation of highly reactive free radicals and unsaturated small fragments in PVC chains. The residence of oxygen in the weather leads to the oxidation of the carbonyl ($-C=O$) groups residues [32]. Therefore, the effect of exposure time to the UV radiation due to the creation of comprising the residues as $-CH=CH-$ (1602 cm^{-1})

and $-C=O$ (1722 cm^{-1}) groups was investigated using FTIR spectroscopy. These band intensities can be observed while being exposed to radiation and contrasted with a related reference peak.

Since UV radiation on the PVC film did not affect the absorption peak at (1328 cm^{-1}), which belonged to the C-H bond, it can be accepted as a reference shown in Figure 7 [33]. After exposure to radiation, the functional group absorption peak intensities increased due to the $-C=C$ and $-C=O$ groups of blank PVC on irradiation in the FTIR spectrum as shown in Figure 7 [35].

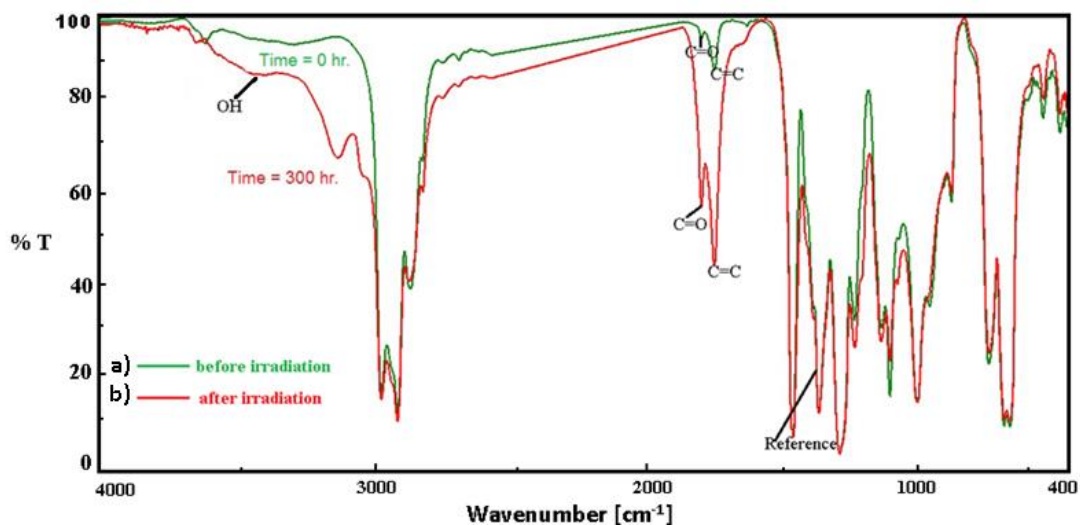


Figure 7: FTIR spectra for blank PVC: (a) before and (b) after irradiation.

Therefore, equation 4 was used to calculate the indices (I_s) of the functional groups of (-CH=CH-, -C=C-, -C=O, and -OH) from the peak of absorbance under study (A_s) and the reference peak (A_r) known as the band index method (Eq. 4) [36].

$$I_s = \frac{A_s}{A_r} \quad (4)$$

Then, equation 5 was applied to determine the absorbance (A) of the functional and reference groups from the transmittance (T).

$$A = 2 - \log T \quad (5)$$

Where, T transmittance (%).

Therefore, the indices $I_{C=C}$, $I_{C=O}$, and I_{OH} were computed for different irradiation times from 50 to 300 h and the results are illustrated in Figures 8-10. Therefore, the influence of irradiation on the indices ($I_{C=C}$), ($I_{C=O}$), and (I_{OH}) are shown respectively. It can be seen from Figures 8-10, that $I_{C=O}$, $I_{C=C}$, and I_{OH} are abundantly advanced about the sample of a thin film of blank PVC. The additives of CNT lead to lower values for $I_{C=O}$, $I_{C=C}$, and I_{OH} to demonstrate their capabilities to decrease the photodegradation of PVC [37].

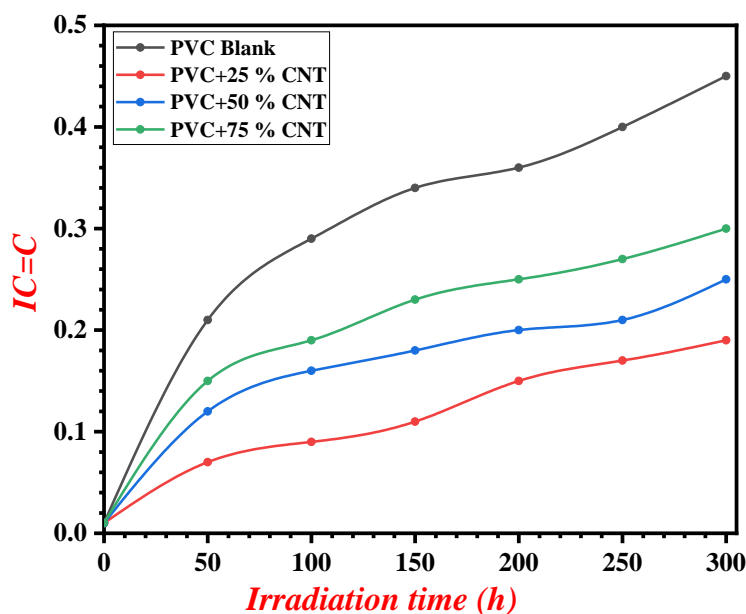


Figure 8: Irradiation time effect on $I_{C=C}$ index for the blank PVC and PVC with CNT blended.

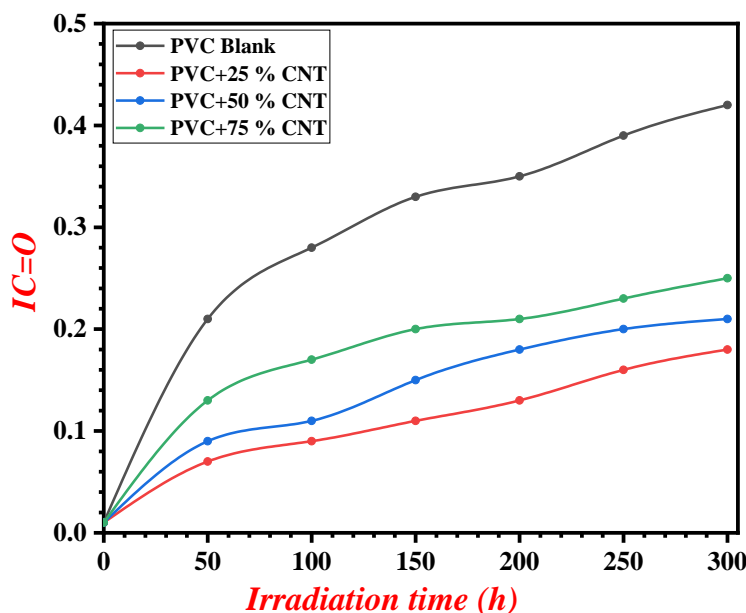


Figure 9: Irradiation time effect of on $I_{C=O}$ index for the blank PVC and PVC with CNT blended.

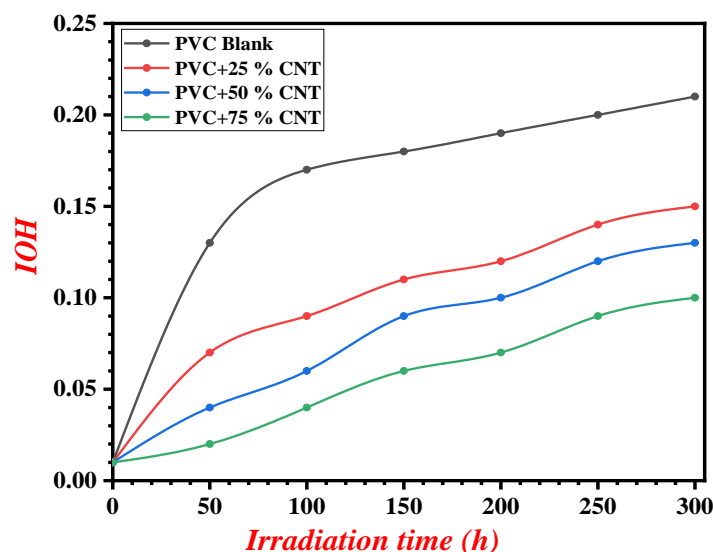


Figure 10: Irradiation time effect on I_{OH} index for the blank PVC and PVC with CNT blended.

It can be seen from Figures 8-10, the nanocomposite thin films (PVC/CNT) showed the lowest $I_{C=O}$, $I_{C=C}$, and I_{OH} . Where, the values of $I_{C=C}$ after 300 h of the irradiation process were 0.17, 0.23, and 0.28 for the thin films containing PVC/0.25 CNT, PVC/0.50 CNT, and PVC/L/0.75 CNT respectively. Similarly, after irradiation of 300 h, the $I_{C=O}$ values were 0.16, 0.2, and 0.24 for the thin films PVC/0.25 CNT, PVC/0.50 CNT, and PVC/L/0.75 CNT respectively. Finally, the values of I_{OH} after irradiation process of 300 h were 0.14, 0.12, and 0.058 for the thin films containing PVC/0.25 CNT, PVC/0.50 CNT, and PVC/0.75 CNT respectively [38, 39].

These indices represented to prolong the extend shelf life of coating for the nanocomposite thin films with CNT to do in applications for long time comparative with the blank PVC, where after adding CNT give these thin films long period for this coating in many applications.

3.6. UV irradiation impact on molecular weight of PVC

There are small fragments that occurred as a product of the chain division and the PVC cross-linking, which led to a decrease in the molecular weight of the PVC. The intrinsic viscosity $[\eta]$ of the PVC is proportional directly to the observed decrease in the average molecular weight viscosity (M_v). The films were then dissolved in THF after the PVC had been exposed to radiation for various lengths of time, and the viscosity of the solutions was assessed using an Ostwald

viscometer. The Mark-Houwink relationship was utilized to derive the calculations for the M_v changes as shown in equation 6 [40]:

$$\eta = 1.63 \times 10^{-2} \times M_v^{0.77} \quad (6)$$

Thereby, Figure 11 shows the relationship of the average molecular weight viscosity (M_v) with the irradiation time from 50-300 h.

Therefore, Figure 11 shows the average molecular weight viscosity (M_v) rises for the coating after addition of the CNT to the PVC lattice, when the coating exposure to the irradiation time and prolong its life.

3.7. UV irradiation impact on external surface morphology of PVC thin film

An inspection of the surface of the thin film after UV irradiation by utilizing a field emission scanning electron microscope (FESEM), to provide information about grooves or white spots to give us the exploiting scan morphology of the UV exposed blank PVC thin film and PVC with CNT as well as the mixed films, which allowed us to provide a description of the surface of the thin films [41]. The FESEM reveals images of the surface that are homogeneous, non-distorted, and transparent, and they contain white spots. The blank PVC film surface that had not been exposed to ionizing radiation was homogenous, smooth, and free of grooves or white spots for the Figures 12 b, 12 c, and 12 d. In opposition, the FESEM picture of the irradiated blank PVC exhibited clear irregularities, grooves for the Figures 12 a and 12 b. Therefore, the

white spots which related to the photodegradation in the thin films of PVC with CNT (Figures 12 b, 12 c, and 12 d) [42].

3.8. Atomic force microscopy

The blank PVC and PVC with CNT surface morphology of samples containing CNT (0.25, 0.50, and 0.75) was observed using atomic force microscopy (AFM). This technique supplies clear 2D and 3D images to explore the flatness of the PVC surfaces irradiated [42]. The long time exposure of the samples to ultraviolet irradiation resulted in bond breaking which appear as roughness and broken surface in blank

PVC [43], while the addition of CNT to the PVC films decrease the cracking, dark spots, and roughness as shown in Table 1 to illustrate the surface roughness and root mean square for the particles. It can see from Figure 13 that the roughness of the samples increases after adding CNT to the PVC lattice, and also decrease the cracking for the samples after exposure to UV irradiation, adding CNT to the PVC structure leads to strengthening the structure and preventing the cracking between bonds [44]. Table 2 AFM test for blank PVC, PVC+ 0.25 CNT, PVC+ 0.50 CNT, and PVC+ 0.75 CNT before and after irradiation.

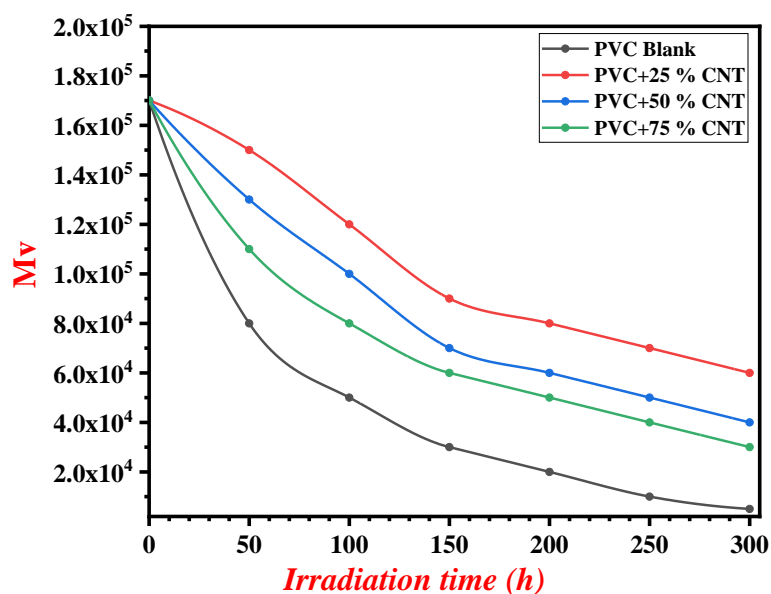


Figure 11: Viscosity of the average molecular weight of the blank PVC and PVC with CNT blended.

Table 2: Roughness average and root mean square for the PVC samples

No.	Composite	Average roughness (nm)	Root mean square of roughness (nm)
1	Blank PVC	3.94	5.84
2	Blank PVC after irradiation	4.83	6.79
3	PVC+ 0.25 CNT	5.19	7.28
4	PVC+ 0.50 CNT	7.69	10.00
5	PVC+ 0.75 CNT	6.79	8.82

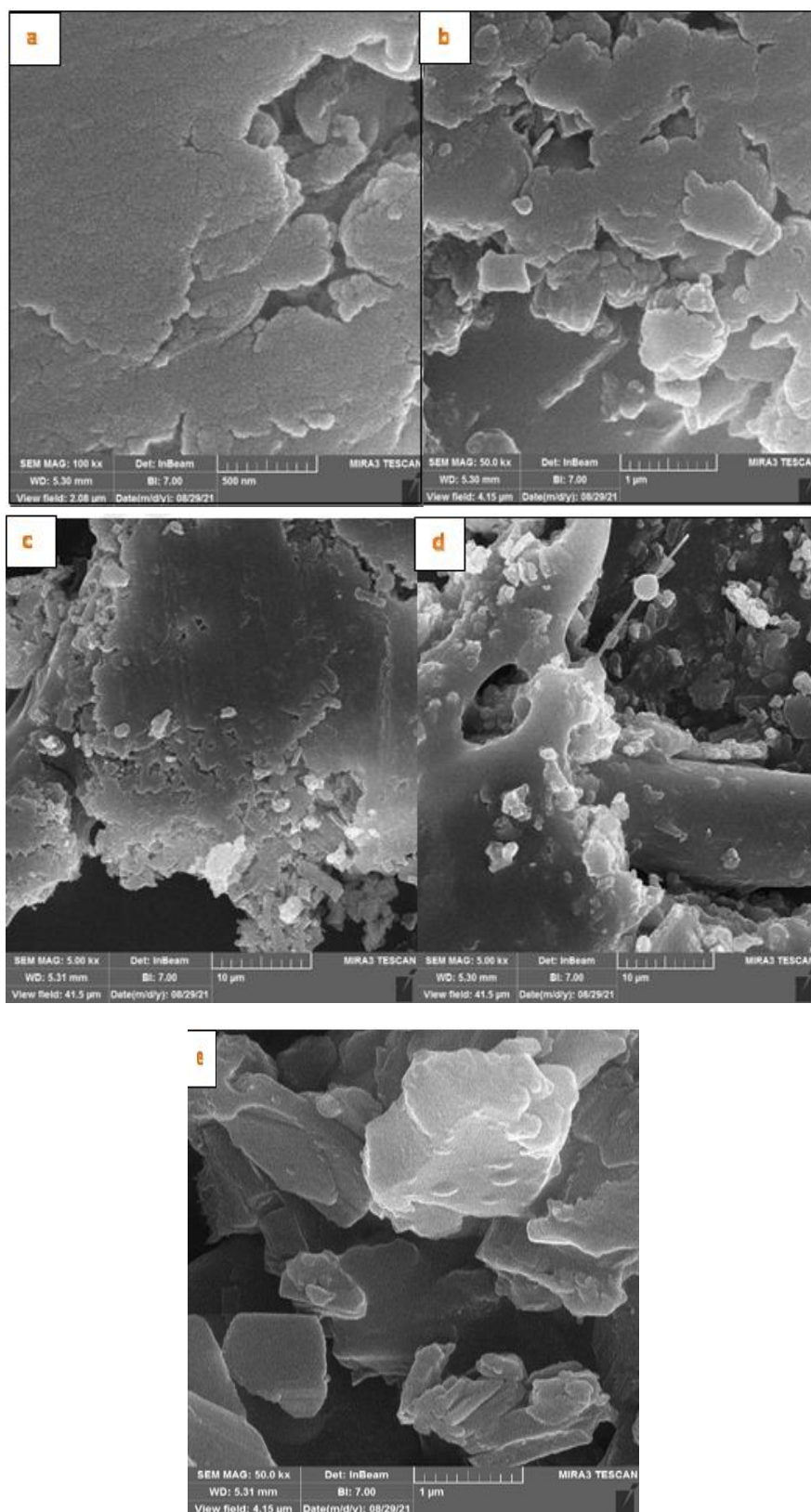


Figure 12: SEM images for a) PVC before radiation, b) PVC after radiation, c) PVC+0.25 after radiation, d) PVC+0.5 after radiation and e) PVC+0.75 after radiation.

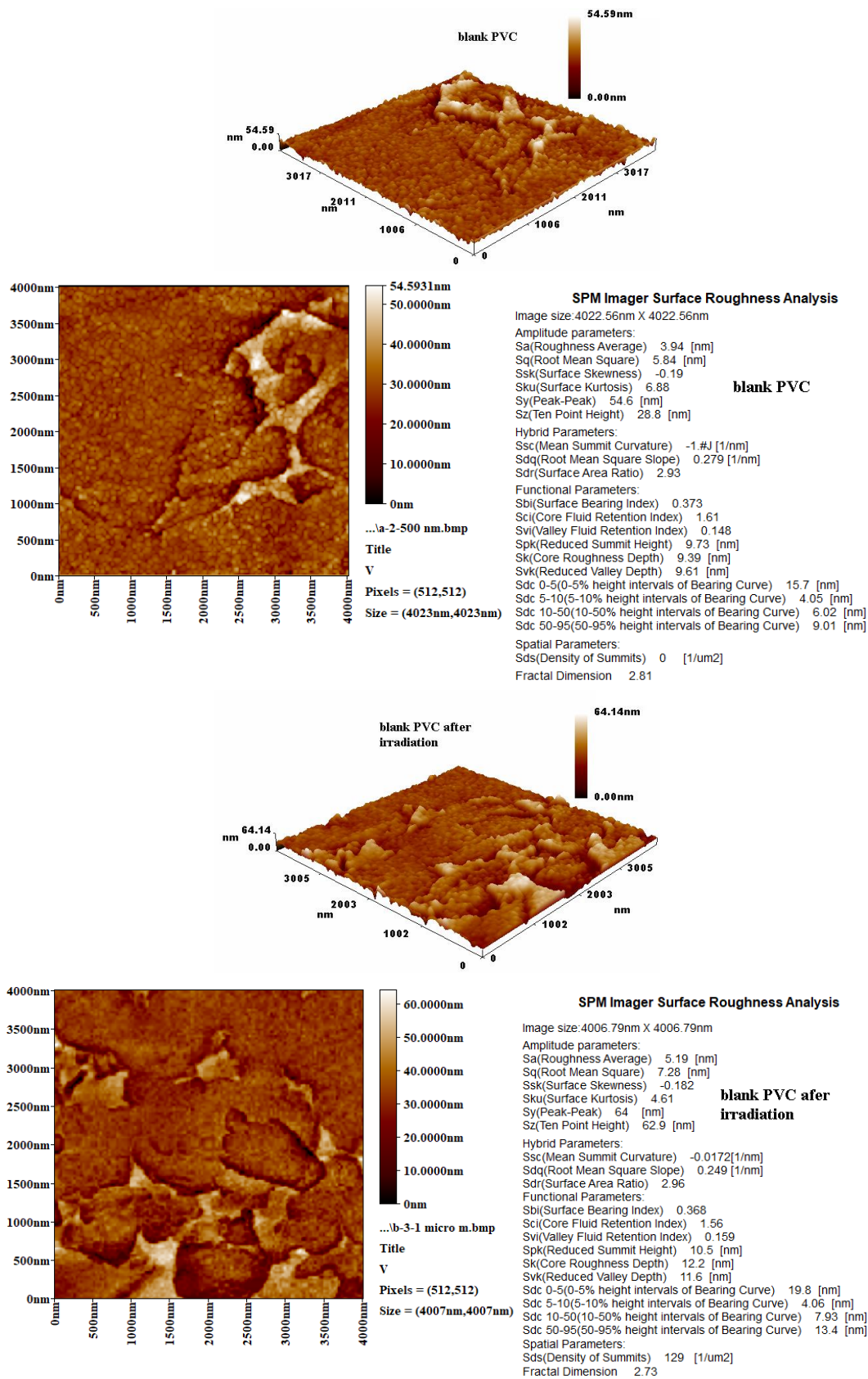


Figure 13: Images of atomic force microscopy (AFM) of irradiation blank-PVC film, blank PVC after irradiation, and PVC with CNT films after irradiation of different concentration.

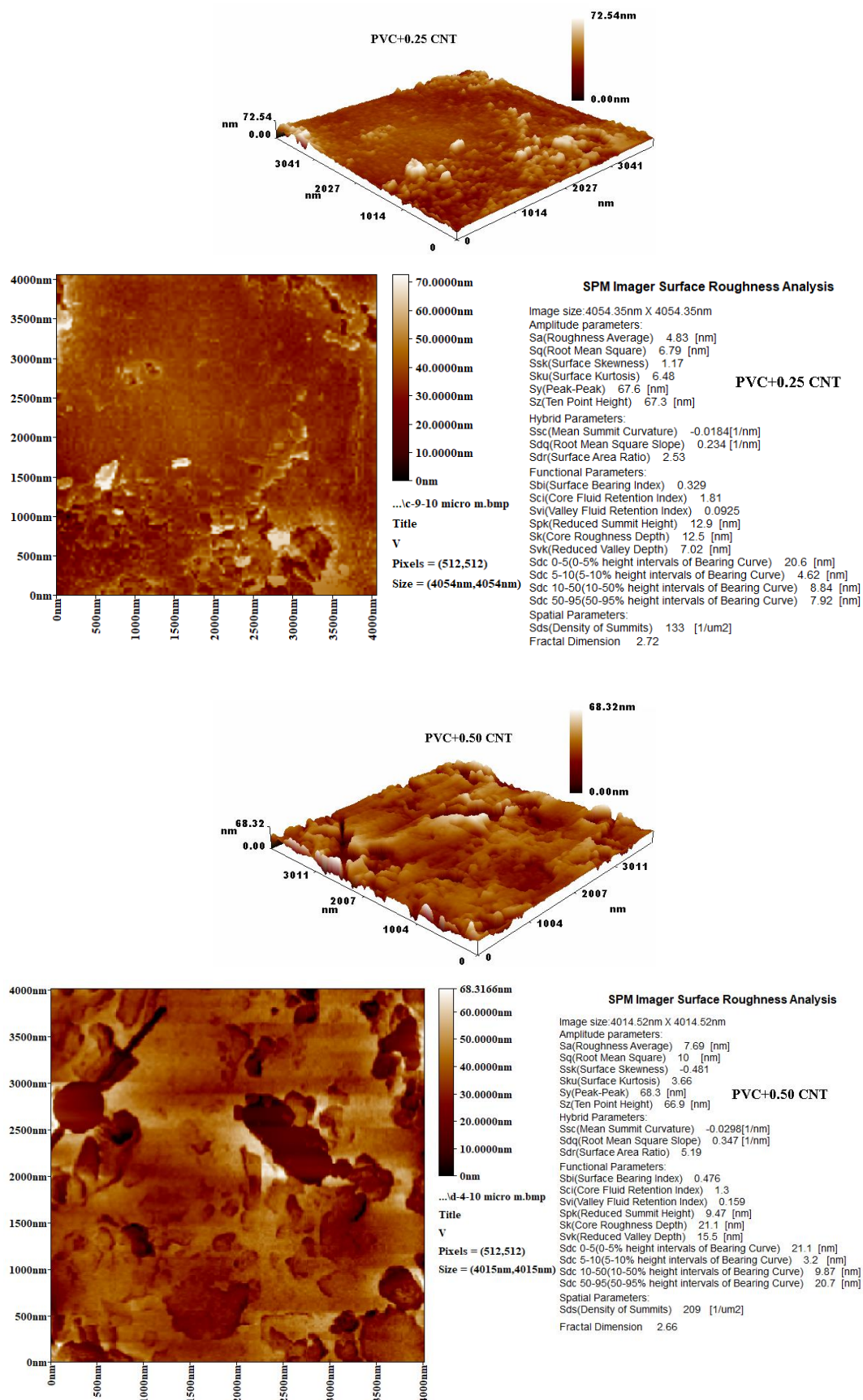


Figure 13: Continue.

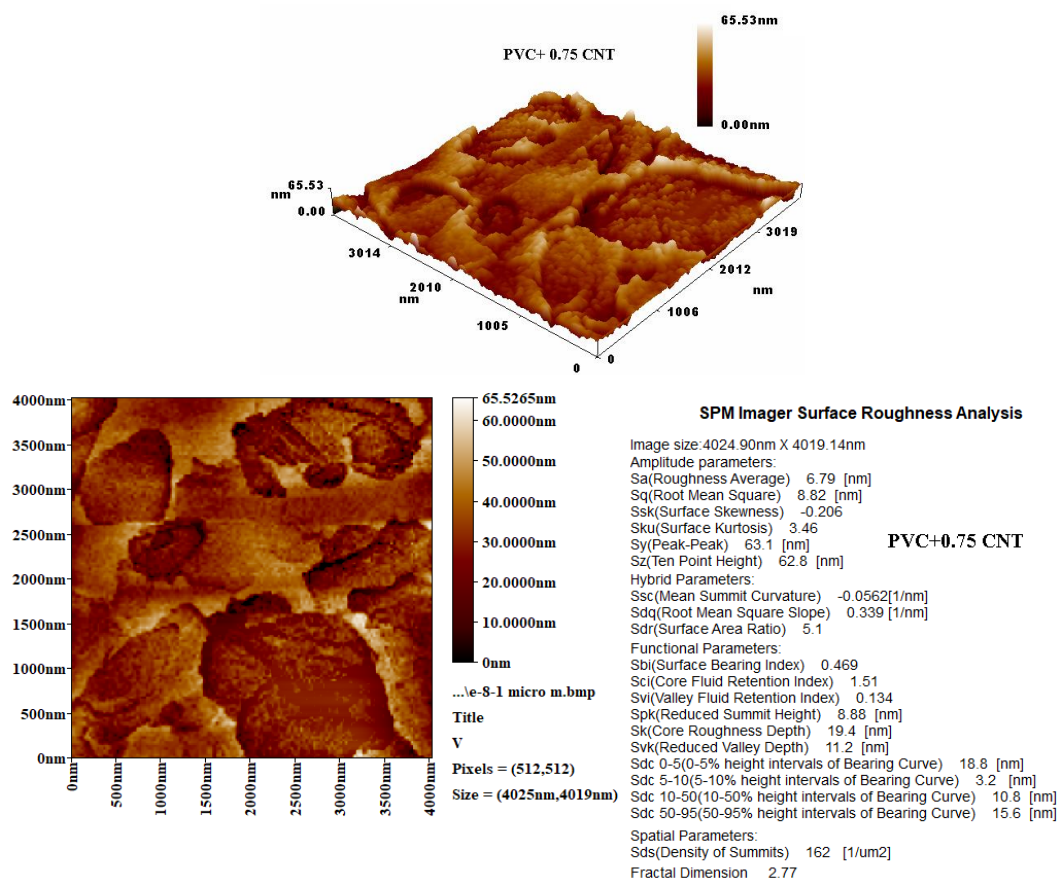


Figure 13: Continue.

4. Conclusion

In the present work, different concentrations of CNT (0.25, 0.50, and 0.75) were added to PVC to constitute thin films. The absorption coefficient for the nanocomposite thin films of PVC/CNT was very high through the UV region, and they have low reflectance. The XRD test was done and its results were used to compute the crystallite size of the nanoparticles and micro-strain. The influence of this additive was followed by the results of carbonyl groups (I_{CO}) between (0.16-0.24), polyene ($I_{C=C}$) between (0.17-0.28), and hydroxyl (I_{OH}) between (0.14-0.58) separately, these indices is regarded as an indication to prolong the extend life coating of the nanocomposite thin films of PVC. The usage applications for the nanocomposite thin films of PVC when compared with the blank PVC have a long life to reserve the coating. The weight loss of the irradiated thin films, and the surface morphology of undesirable changes were much less after adding CNT nanoparticles. In addition, both the weight loss and viscosity of the thin films were also examined to investigate the photostability, then found

that the weight loss decreased and the viscosity increased after adding CNT. The images of SEM exhibited the PVC structure shape before and after exposed to UV light. It was found that the photodegradation of the PVC films was decreased with raising the CNT concentration and the increasing the photostability followed the order below: (PVC+0.75) > (PVC+0.50) > (PVC+0.25) > (PVC). The samples surface roughness were examined by an AFM device which exhibited the increases in roughness after adding CNT to the PVC lattice to avoid cracking and distortion to the bonds that happen in the PVC structure, where, the average roughness was 4.83 nm for PVC blank, and the average roughness increases after adding CNT to become between (5.19-7.69 nm). The nanocomposite thin films of PVC with CNT are used in many applications such as electronics, automobile components, medical products, office equipment, sports materials, plastic cards, packaging, and outdoor applications such as cables cover, fittings of piping in electricity.

Acknowledgment

This work was supported by Polymer Research Center/ College of Science of Al-Mustansiriyah University,

Middle technical University/ Institute of Technology, and Department of Mechanical Engineering/College of Engineer/ Al-Nahrain University.

5. References

- Lewandowski K, Skórczewska K. A brief review of poly(vinyl chloride) (PVC) recycling. *Polymers*. 2022; 15: 3035, 1-14. <https://doi.org/10.3390/polym14153035>.
- Akl AA, El Radaf IM, Hassanien AS. Intensive comparative study using X-Ray diffraction for investigating microstructural parameters and crystal defects of the novel nanostructural ZnGa₂S₄ thin films. *Superlatt Microstruct*. 2020; 143: 106544. <https://doi.org/10.1016/j.spmi.2020.106544>.
- El Radaf IM, Hassanien AS. Effect of thickness on structural, optical, and optoelectrical properties of sprayed CuInSnS₄ thin films as a new absorber layer for solar cells, *Phys B: Cond Matter*. 2023; 659: 414867. <https://doi.org/10.1016/j.physb.2023.414867>.
- Akl AA, Hassanien AS. Comparative microstructural studies using different methods: Effect of Cd-addition on crystallography, microstructural properties, and crystal imperfections of annealed nano-structural thin Cd_xZn_{1-x}Se films. *Phys B: Phys Cond Matter*. 2021; 620: 413267. <https://doi.org/10.1016/j.physb.2021.413267>.
- Abdullah SM, Alwan AF, Majeed AM. The Influence of the UV light on the PVC sheets adopted with some aromatic amines, *ANJS*. 2022; 25: 9-13. <https://doi.org/10.22401/ANJS.25.1.02>.
- Yousif E, Hasan A. Photostabilization of poly(vinyl chloride) – Still on the run. *J Taibah Univ Sci*. 2015; 4: 421-448. <http://dx.doi.org/10.1016/j.jtusci.2014.09.007>.
- El-Denglawey A, Aly KA, Dahshan A, Hassanien AS. Optical characteristics of thermally evaporated thin a-(Cu₂ZnGe)_{50-x}Se_{50+x} films. *ECS J Solid-State Sci Techn*. 2022; 11: 044006. <https://doi.org/10.1149/2162-8777/ac627b>.
- Saleh TAK, Al-Tikrity ET, Yousif E, Al-Mashhadani MH, Jawad AH, Preparation of schiff bases derived from chitosan and investigate their photostability and thermal stability. *Phys Chem Res*. 2022; 10: 549-557. <http://dx.doi.org/10.22036/PCR.2022.333808.2051>.
- Shalan N, Laftah N, El-Hiti GA, Alotaibi MH, Muslih R, Ahmed DS, Yousif E. Poly(vinyl Chloride) photostabilization in the presence of schiff bases containing a thiadiazole moiety. *Molecules*. 2018; 23(4):913.<http://dx.doi.org/10.3390/molecules23040913>.
- Sa'aedi A, Akl AA, Hassanien AS. Effective role of Rb doping in controlling the crystallization, crystal imperfections, and microstructural and morphological features of ZnO-NPs synthesized by the sol-gel approach. *Cryst Eng Comm*. 2022; 24: 4661-4678. <https://doi.org/10.1039/D2CE00483F>.
- Mohammed SA, Yusop RM, Mohammed MA, Abed RN, Ahmed DS, Ahmed AA, Ahmed A, Ali B, Yousif E. Additives aid switch to protect the photodegradation of plastics in outdoor construction. *NJES*. 2019; 22: 277-282. <http://doi.org/10.29194/NJES.22040277>.
- Alhaydary E, Yousif E, Al-Mashhadani MH, Ahmed DS, Jawad AH, Bufaroosha M, Ahmed AA. Sulfamethoxazole as a ligand to synthesize di-and tri-alkyltin (IV) complexes and using as excellent photostabilizers for PVC. *J Polym Res*. 2021; 28: 1-19. <https://doi.org/10.1007/s10965-021-02822-5>.
- Akl AA, El Radaf IM, Hassanien AS. An extensive comparative study for microstructural properties and crystal imperfections of Novel sprayed Cu₃SbSe₃ Nanoparticle-thin films of different thicknesses. *Optik*. 2020; 227: 165837. <https://doi.org/10.1016/j.ijleo.2020.165837>.
- Al-Mashhadani MH, Salman EA, Husain AA, Abdallah M, Bufaroosha M, Yousif E. Utilizing organic aromatic melamine moiety to modify poly(vinyl chloride) chemical Structure and micro CuO that plays an important role to enhance its photophysical features. *Indones J Chem*. 2022; 22(6): 1187-1194. <http://dx.doi.org/10.22146/ijc.70263>.
- Shnawa HA, Khalaf MN, Jahani Y, Taobi AAH. Efficient thermal stabilization of polyvinyl chloride with tannin-Ca complex as bio-based thermal stabilizer. *Mater Sci Appl*. 2015; 6: 360-372. <http://dx.doi.org/10.4236/msa.2015.65042>.
- Abdullah AM, Alwan LH, Ahmed AA, Abed RN. Physical study of PVA filled with carbon nanotube and nano carbon with roughness morphology. *J Phys Chem Res*. 2023; 11: 747-760. <http://dx.doi.org/10.22036/PCR.2022.362088.2195>.
- Yousif E, Hasan A, El-hiti GA. Spectroscopic, physical and topography of photochemical process of PVC films in the presence of schiff base metal. Complexes. 2016; 8: 204, 1-13. <https://doi.org/10.3390/polym8060204>.
- Abed RN, Yousif E, Abed ARN, Rashad AA. Synthesis thin films of poly(vinyl chloride) doped by aromatic organosilicon to absorb the incident light. *Silicon*. 2022; 14: 11829-11845. <https://doi.org/10.1007/s12633-022-01893-3>.
- Abed RN, Abed ARN, Abed AN. Electrical conductivity of carbon ash surface immersed with nanoparticles (Co₃O₄-Cr₂O₃) for spectroscopic selective surfaces. *Poly Bull*. 2023; 80: 11207-11224. <http://dx.doi.org/10.1007/s00289-022-04601-8>.

20. Hassanien AS, Aly KA, Elsaedy HI, Alqahtani A. Optical characterization and dispersion discussions of the novel thermally evaporated thin $a\text{-S}_{50-x}\text{Ge}_{10}\text{Cd}_x\text{Te}_{40}$ films. *Phys A*. 2022; 128: 1021. <https://doi.org/10.1007/s00339-022-06127-2>.
21. Hadi AG, Jawad K, El-Hiti GA, Alotaibi MH, Ahmed AA, Ahmed DS, Yousif E. Photostabilization of poly(vinyl chloride) by organotin(IV) compounds against photodegradation. *Molecules*. 2019; 24:3557. <https://doi.org/10.3390/molecules24193557>
22. Abdullah AM, Alwan LH, Ahmed AA, Abed RN. Optical and physical properties for the nanocomposite poly(vinyl chloride) with affected of carbon nanotube and nano carbon. *Prog Color Colorant Coat*. 2023; 16(3): 331-345. <https://doi.org/10.30509/PCCC.2023.167082.1198>
23. Hassanien AS. El Radaf IM. Effectiveness of Sn-addition on optical properties and physicochemical parameters of $\text{Sn}_x\text{Sb}_{2-x}\text{Se}_3$ thin films. *Mater Chem Phys*. 2023; 303: 127827. <https://doi.org/10.1016/j.matchemphys.2023.127827>.
24. Ajayan PM, Vajtai R. Properties and applications of carbon nanotubes, *J Carbon Filaments Nanotub Common Orig Differing Appl*. 2001; 32: 315-330. https://doi.org/10.1007/978-94-010-0777-1_23.
25. Hassanien AS, Akl AA, El Redaf IM. Optical characteristics of the novel nanosized thin ZnGa_2S_4 films sprayed at different deposition times: Determination of optical band-gap energy using different methods, *Emerg. Mater*. 2023; 6: 943-964. <https://doi.org/10.1007/s42247-023-00493-0>
26. Hassanien AS, El Radaf IM. Effect of fluorine doping on the structural, optical, and electrical properties of spray deposited Sb_2O_3 thin films. *Mater Sci Semicond Process*. 2023; 160: 107405. <https://doi.org/10.1016/j.mssp.2023.107405>.
27. Saleh TA, Al-Tikrity ETB, Ahmed DS, El-Hiti GA, Kariuki BM, Yaseen AA, Ahmed A, Yousif E. Monitoring physicochemical properties of transparent PVC films containing captopril and metal oxide nanoparticles to assess UV blocking. *J Poly Res*. 2022; 29: 249. <https://doi.org/10.1007/s10965-022-03097-0>.
28. Abdel-Fattah E, Alharthi AI, Fahmy T. Spectroscopic, optical and thermal characterization of polyvinyl chloride-based plasma-functionalized MWCNTs composite thin films. *Appl Phys A*. 2019; 125: 475. <https://doi.org/10.1007/s00339-019-2770-y>
29. Abed RN, Abed ARN. Characterization effect of copper oxide and cobalt oxide nanocomposite on poly(vinyl chloride) doping process for solar energy applications. *Prog Color Colorants Coat*. 2022; 15(2): 235-241. <https://doi.org/10.30509/PCCC.2021.166858.1123>.
30. Omer RM, Al-Tikrity ETB, Abed RN, Kadhom M, Jawad AH, Yousif E. Electrical conductivity and surface morphology of PVB films doped with different nanoparticles. *Prog Color Colorants Coat*. 2022; 15(3): 191-202. <https://doi.org/10.30509/PCCC.2021.166839.1120>.
31. Abed RN, Al-Sahib NK, Khalifa AJN. Energy gap demeanor for carbon doped with chrome nanoparticle to increase solar energy absorption. *Prog Color Colorants Coat*. 2020; 13(2): 143-154. <https://doi.org/10.30509/PCCC.2020.81613>.
32. Salam B, El-Hiti GA, Bufaroosha M, Ahmed DS, Ahmed A, Alotaibi MH, Yousif E. Tin complexes containing an atenolol moiety as photostabilizers for poly(vinyl chloride). *Polymers*. 2020; 12: 2923. <https://doi.org/10.3390/polym12122923>.
33. Silvano, LT, Vittorazzo AL, Araujo RG. Effect of preparation method on the electrical and mechanical properties of PVC/Carbon nanotubes nanocomposites. *Mater Res*. 2018; 21: 1-6. <https://doi.org/10.1590/1980-5373-MR-2017-114.8>.
34. jasim B, husain A, aboud N, Rheima A. Aqueous solution decolorization utilizing low cost activated carbon. *Egyptian J Chem*. 2022; 65: 1395-1400. <https://doi.org/10.21608/EJCHEM.2022.152591.6610>.
35. Akl AA, Hassanien AS. Microstructure characterization of Al-Mg alloys by X-ray diffraction line profile analysis. *Inter J Adv Res*. 2014; 2: 1-9. https://www.journalijar.com/uploads/838_IJAR-4360.pdf130,1-14.
36. Medhat A, El-Maghrabi HH, Abdelghany A, Abdel-Menem NM, Raynaud P, Moustafa YM, Elsayed MA, Nada AA., Efficiently activated carbons from corn cob for methylene blue adsorption. *Appl Surf Sci Adv*. 2021; 3: 100037. <https://doi.org/10.1016/j.apsadv.2020.100037>.
37. Abed RN, Sattar MA, Hameed SS, Ahmed DS, Al-Baidhani M, Kadhom M, Jawad AH, Zainulabdeen K, Al-Mashhadani MH, Rashad AA, Yousif E. Optical and morphological properties of poly(vinyl chloride)-nano-chitosan composites doped with TiO_2 and Cr_2O_3 nanoparticles and their potential for solar energy applications. *Chem Papers*. 2023; 77: 757-769. <https://doi.org/10.1007/s11696-022-02512-6>.
38. Hassanien AS, Sharma I, Sharma P. Inference of Sn addition on optical properties of the novel thermally evaporated thin $a\text{-Ge}_{15}\text{Te}_{50}\text{S}_{35-x}\text{Sn}_x$ films and some physical properties of their glasses. *Mater Chem Phys*. 2023; 293: 126887. <https://doi.org/10.1016/j.matchemphys.2022.126887>.
39. Sharma I, Sharma P, Hassanien AS. Optical properties and optoelectrical parameters of the quaternary chalcogenide amorphous $\text{Ge}_{15}\text{Sn}_x\text{S}_{35-x}\text{Te}_{50}$ films. *J Non-Crys Solids*. 2022; 590: 121673. <https://doi.org/10.1016/j.jnoncrysol.2022.121673>
40. Mark JE. *Physical properties of polymers handbook*. Springer, New York, 2007; pp. 17-26. <https://doi.org/10.1007/978-0-387-69002-5>.
41. Venkateshaiah A, Padil VVT, Nagalakshmaiah M, Waclawek S, Cernik M, Varma, RS. Microscopic techniques for the analysis of micro and nanostructures of biopolymers and their derivatives. *Polymers (Basel)*. 2020; 12: 512. <https://doi.org/>

- 10.3390/polym12030512.
42. Al-Mashhadani MH, Thamer H, Adil H, Ahmed A, Ahmed DS, Bufaroosha M, Jawad AH, Yousif E. Environmental and morphological behavior of polystyrene films containing schiff base moiety. *Mater Today Proc.* 2021; 42: 2693-2699. <https://doi.org/10.1016/j.matpr.2020.12.706>.
43. Abed RN, Yousif E, Abed ARN, Rashad AA, Hadawey A, Jawad AH. Optical properties of PVC composite modified during light exposure to give high absorption enhancement. *J Non-Crys Solids.* 2021; 570: 120946. <https://doi.org/10.1016/j.jnoncrysol.2021.120946>.
44. Tanrikulu EE, Variation of electrical and dielectric characteristics of Schottky diodes (SDs) depending on the existence of PVC and carbon-nanotube (CNT)-doped PVC interlayers. *J Mater Sci. Mater Electron.* 2023; 34: 63. <https://doi.org/10.1007/s10854-022-09479-w>

How to cite this article:

Dadoosh RM, Alwan AF, Farhan SA, Essam Jassim B, Mahmood A, Ghaeb Al-Saadi L, Abed RN. Study of Physicochemical Properties of PVC Thin Films Affected by Carbon Nanotubes to Prevent Photodegradation During UV Light Exposure. *Prog Color Colorants Coat.* 2024;17(3):307-324. <https://doi.org/10.30509/pccc.2024.167260.1275>.

